Chapter 5a
Effect of ethanol as molecular crowding agent on the conformational dynamics of α-Synuclein

Effect of ethanol as molecular crowding agent on the conformational dynamics of α-Synuclein

5a.1. Abstract:

The functions of many proteins have been directly connected to their conformational changes. The macromolecular crowding environment inside the cell is known to have a significant impact on the equilibria and transition rates between different conformations of the protein. Here we demonstrate the effect of ethanol as crowders on the conformational dynamics of α-Syn protein, a primary component of the fibrillar neuronal inclusions, and known as LB that are diagnostic of PD. We observed the α-Syn protein to experience stronger crowding effects with an increase in concentration of ethanol, the crowding agent. The findings that we obtained from this simulation study would serve as valuable guides for expected crowding effects on conformational dynamics of α-Syn.

5a.2. Introduction:

In the recent past, many research studies have highlighted the importance of the protein dynamics as a valuable platform to understand the association between the structures and function [344-349]. The protein dynamics leads to the sampling of alternative conformations. Because of ligand binding [350] and post-translational modifications like phosphorylation [351], the conformational changes in the protein molecule gets initiated. As a result, the protein molecule adopts different conformations at varying functional states. From these structures, the conformational changes at atomistic level can be studied. We generally see that biophysical characterizations of conformational changes in protein have been studied mostly under dilute and lesser densed medium. But the proteins perform their biological functions inside the cell which is highly crowded with macromolecules. For example, the cytoplasm of *Escherichia coli* contains high concentration of macromolecules (about 300–400 g/l and 30% of the total volume occupancy) [352]. Because of crowding in cell membranes, membrane proteins occupy a similar level of the total surface area [353]. However, the impact of crowding environment in cell on the equilibria and transition rates of diverse conformations of proteins are not understood well [354]. Such effects of crowding have been verified experimentally [351]. MD simulations have also been used as a tool to investigate the energy landscapes of a number of proteins in a crowding environment, in the context of either conformational change [355] or folding-unfolding transition [356-358]. In our study, we have investigated the consequences of ethanol as a crowding medium on the conformational dynamics of α-Syn. We have found the

crowding environment to affect the secondary structure content of α-Syn to a greater extent.

5a.3. Materials and Methods:

5a.3.1.Preparation of the initial structure:

The initial 3-D structure of α-Syn was taken from PDB [252].

5a.3.2. Preparation of the crowding agent:

The volume occupied by ethanol was set up to about 0%, 5%, 10%, 20%, 50% and 100% of total volume. In carrying out this experiment, cubic simulation boxes were filled with different proportions of water-ethanol mixtures using Packmol.

5a.3.3. Setup for MD simulation:

In order to study the effect of different concentrations of ethanol, the crowding agent on the conformational dynamics of α-Syn, we have employed MD simulation using the explicit solvent model. MD simulations were performed using periodic boundary conditions. In all these cases, the protein molecule was placed at the center of the simulation box using Leap module of AmberTools 14 program. The protein molecules are then overlaid by equilibrated TIP3P boxes in order to solvate the molecule of interest in the respective cubic simulation boxes. In addition, positively charged Na+ counter-ions were added into the system to neutralize the negative charge on the protein molecules. To study the structural dynamics of IDP, MD simulations have been extensively in use. The AMBER14 package was used to perform MD simulation while protein and water molecules are described by parameters from ff99SB force field and TIP3P water molecules in the system. In each system, the charge of the protein was neutralized by adding Na+/Cl- counter ions. An isobaric–isothermal ensemble was applied using Langevin dynamics [359] along with Berendsen- thermostat [360] for temperature control. The system was subjected to one stage minimization to ensure the stability of the structure. The integration time step was set to 1 fs. To further take the system to room temperature, heating was gradually performed to bring the temperature of the system to 298 K over a time of 10 ps.

5a.3.4. Analysis of MD trajectories:

To ensure the equilibration of the system, pressure, density, temperature, RMSD, potential energy, kinetic energy and total energy of the initial structure of α-Syn were plotted as a function of simulation time. The trajectories were collected and visualized by VMD [361] package after

intervals of 10ns for a total MD run of 50 ns and analysed using cpptraj [362] program from AMBER tools [205].

5a.4. Results and Discussions:

In order to compare the conformational dynamics of α-Syn in different concentrations of ethanol, we carried out all atom MD simulation using the PMEMD module of AMBER14 software package with ff99SB force field.

Our results demonstrate that α-Syn folds in a multiphasic manner in the presence of ethanol as a crowding agent. We noticed the folding pathway of α-Syn to vary with the concentration of ethanol. Although the mechanism of folding changes with the concentration of ethanol, yet it was characterized by a common first stage that actually leads to the partially folded intermediate [363-367]. The nature of the solvent is responsible to decide for the subsequent fate of this intermediate. It has been seen that the higher concentrations of ethanol gave rise to α-helical conformation. These observations infer that, depending on the environment, the partially folded intermediate may undergo self-association to form dimers, soluble oligomers or amorphous aggregates and fibrils. We also observed that α-Syn in higher concentrations of ethanol revealed significant ordered secondary structure The capacity of concentrated organic solvent inducing the structural changes in the native globular proteins have been reported. Typically, alcohol-induced denaturation of globular proteins is accompanied by a characteristic increase in α-helix content [368-381]. Much less is currently known about the behaviour of natively unfolded proteins in water/organic mixtures [257,382,383]; however, one would expect similar effects. The structural transformations and oligomerization of α-Syn in simple alcohols were driven by the increase in solvent hydrophobicity. These results, therefore, exclude contributions from specific protein alcohol interactions, indicating that water/alcohol mixtures might be useful models for the effect of hydrophobic membrane surfaces (the membrane field effect) on the conformation of α-Syn and other natively unfolded proteins.

5a.4.1. Conformational dynamics of α-Synuclein in different concentrations of crowding agent:

To study the conformational dynamics of α-Syn in different concentrations of ethanol, the crowding agent, we have analyzed the RMSDs of the Cα atoms, Rg, RMSF and SASA over the course of simulation time as shown in **Figure 5a.1.** Assessment of the structural drift was carried out by analyzing the Cα atom RMSDs. We observed the RMSD profile in each case of the protein to be varying **(Figure 5a.1 (A))**. The backbone RMSD of the protein attained almost stable conformation from the initial stage in case of 100% ethanol whereas in case of 0%, 5%,

10%, 20%, 50% ethanol the structure had undergone conformational changes through the initial time period of around 4.5 ns, 4.5 ns, 4 ns, 2.5 ns and 2 ns respectively, and then reached equilibration. RMSD value of α-Syn in 100% ethanol corresponds to 7.5 Å, 50% ethanol is 11 Å, 20% ethanol is 13 Å, 10% ethanol is 15 Å, 5% ethanol is 19 Å and 0% ethanol is 21 Å. From these RMSD analyses we can infer that α-Syn reaches equilibration very quickly with an increase in concentration of crowding. The stability of the protein is due to its ability to retain its native α-helical conformation even at higher concentration of ethanol.

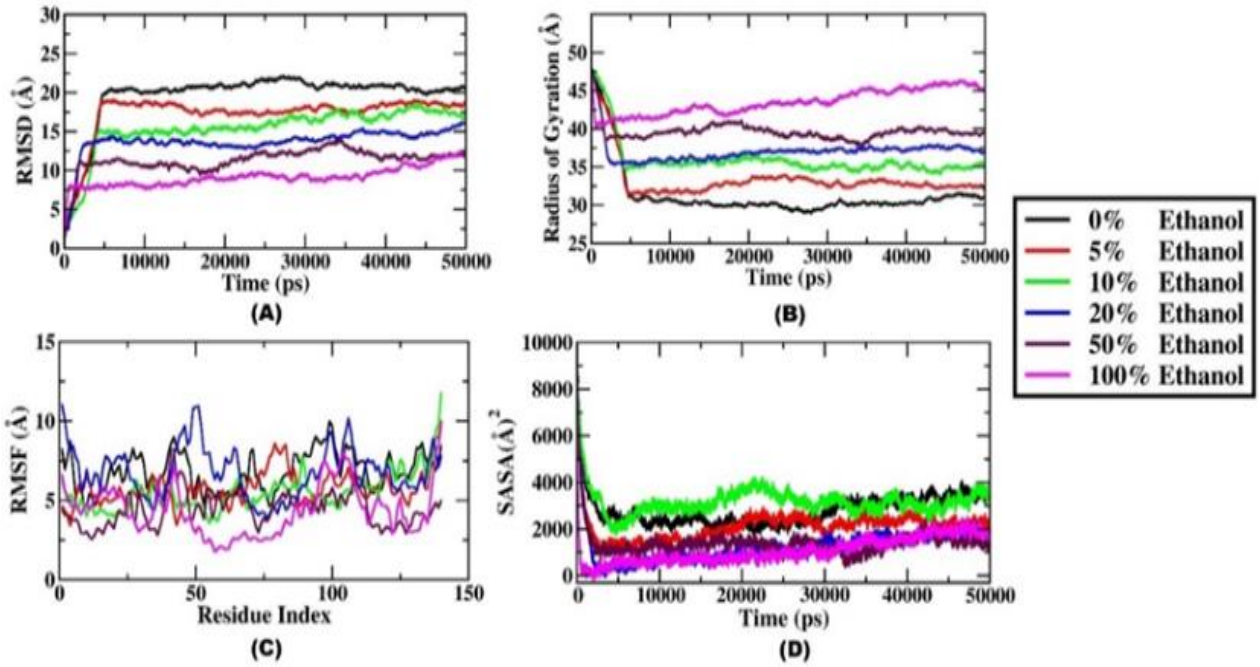

Figure 5a.1. *Comparative MD analyses of (A) RMSD, (B) Rg, (C) RMSF and (D) SASA, for α-Syn in different concentration of ethanol*

Figure 5a.1 (B) shows the radius of gyration analysis of α-Syn protein as a function of time. In the simulation carried out, the radius of gyration oscillated to a greater degree before 2 ns, further confirming that the peptide structure remained stable after 2 ns from the simulation being initiated. From the Rg plots, we can see that with an increase in ethanol concentration, the structure of α-Syn was found to be less compact. The size of the molecule was bigger in a higher concentration of ethanol. α-Syn in 100% ethanol depicts the highest Rg value as observed from the plot. So, it can be inferred that α-Syn retains its structure having more helical content in the higher crowding environment that makes it lesser prone to aggregation. Thus, it is evident that the aggregation propensities of α-Syn decreases with increasing proportions of ethanol. To obtain information on local structural flexibility, thermal stability and heterogeneity of macromolecules, RMSF of α-Syn were studied **(Figure 5a.1 (C))**. RMSF values obtained for

the backbone C-α atom in different concentrations of ethanol were calculated from the corresponding MD simulation trajectories and were plotted against their residue numbers. It can be inferred from the plot that fluctuation in conformational dynamics of α-Syn was found to decrease with an increase in ethanol concentration. In order to get information regarding the buried and exposed area present in the protein structure, SASA analysis was carried out (**Figure 5a.1 (D)**). The overall solvent accessible area of the protein molecule was analyzed in different concentrations of ethanol.

From **Figure 5a.1(D)**, it can be seen that α-Syn in 0% ethanol has higher SASA values while in 100% ethanol the SASA value was found to decrease. The SASA of α-Syn decreases with an increase in the ethanol concentration.

5a.4.2. Secondary Structural Analysis of α-Synuclein in different concentrations of crowding agent:

The secondary structure analysis was carried out for α-Syn in the crowding medium using the Kabsch and Sander algorithm incorporated in their DSSP program [295]. The probability score graph results were in good agreement with the assessment that crowding supports in retaining the native structure of α-Syn. (**Figure 5a.2**). From the graph we can observe that most of the residues retained their α-helical conformation in presence of 100% ethanol.

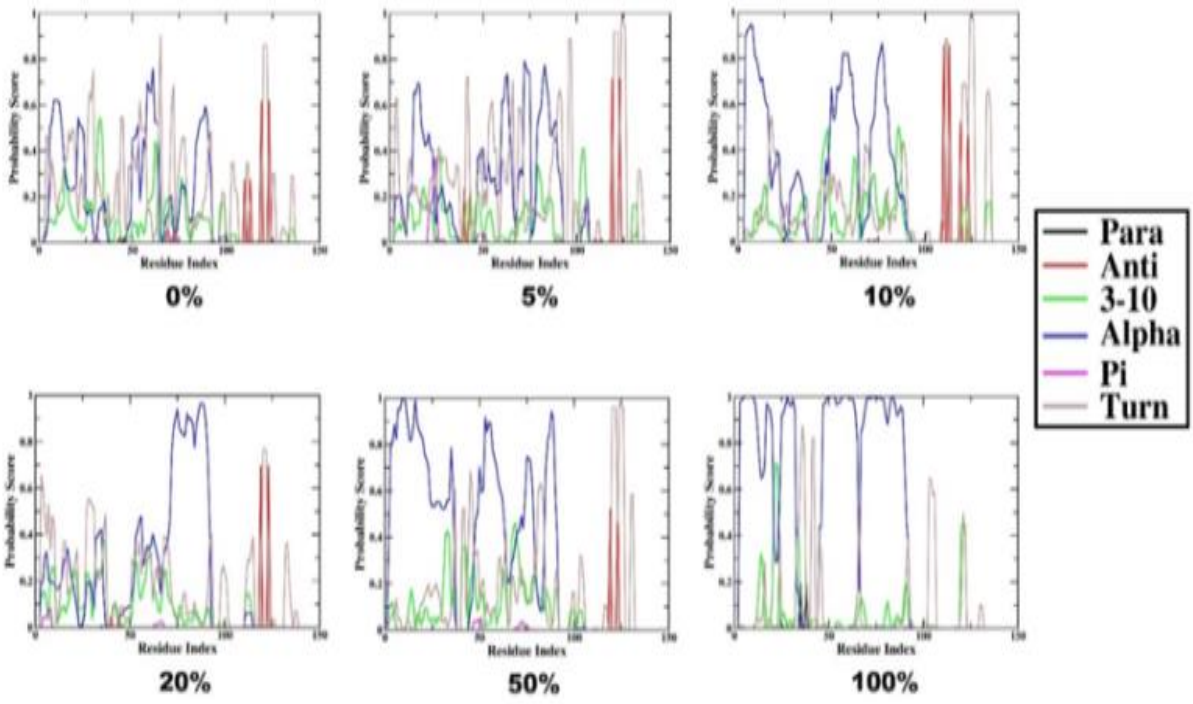

Figure 5a.2.*Probability score of secondary structure for each residue in α-Syn in 0%, 5%, 10%, 20%, 50% and 100% ethanol concentration*

The plot shows the secondary structural variation of each residue during the course of simulation time. In each case, the alpha helical portion of the structure was increased with an increase in concentration of ethanol, the crowding medium. The protein in 100% ethanol tends to have higher helical content in comparison to other proportions. So, the existence and rapid changes in structural dynamics of α-Syn in crowding media were clearly visible from secondary structure analysis.

We also calculated the percentage of individual secondary structure content in α-Syn across all conformations using YASARA software [257] that were sampled during the production job of trajectories and the results were summarized in **Table 5a.1**. From **Table 5a.1**, we observed that α-Syn in 100% ethanol contains a higher amount of α-helix than the other systems. So, these observations support that higher helical conformation in α-Syn which is predominant in case of 100% ethanol, to be actually responsible for preventing fibrillation process as this structural characteristic feature would induce a similar conformation that restricts fibrillation as proposed earlier.

Table 5a.1. *Secondary structure content of α-Syn in 0%, 5%, 10%, 20%, 50% and 100% ethanol*

Concentration of Ethanol	α-helix %	β-sheet %	turn %	Coil %	3_{-10} helix %	Pi-helix %
0%	4.3%	0.0%	34.3%	61.4%	0.0%	0.0%
5%	8.6%	0.0%	37.1%	54.3%	0.0%	0.0%
10%	5.0%	1.4%	30.0%	60.0%	3.6%	0.0%
20%	22.1%	0.0%	8.6%	63.6%	5.7%	0.0%
50%	20.0%	2.1%	30.0%	47.9%	0.0%	0.0%
100%	55.0%	0.0%	5.7%	39.3%	0.0%	0.0%

Figure 5a.3 shows the classification of the trajectories in terms of secondary-structure elements obtained by the software tool DSSP which assigns secondary structures to the amino acids of a protein, by identifying the intra-backbone hydrogen bonds of the protein. From the plot we can see the stability (or de-stability) of secondary structure elements as a function of time. Examination of **Figure 5a.3** shows that the main features of the α-helix structure were largely retained in the case of 100% ethanol as compared to other systems.

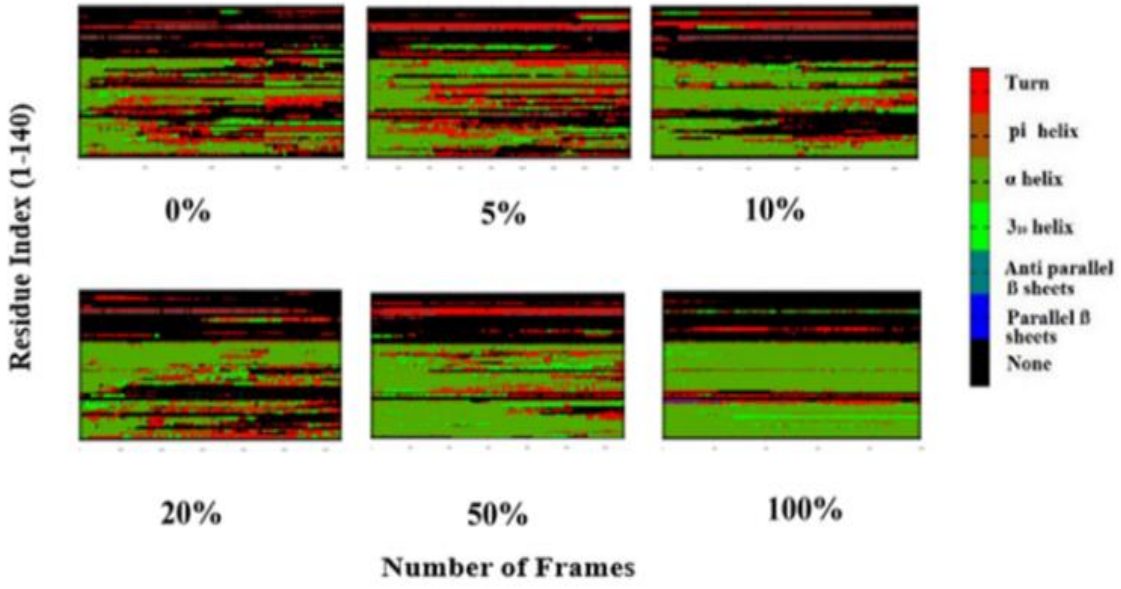

Figure 5a.3. *Time evolution of Secondary structure of α-Syn in presence of 0%, 5%, 10%, 20%, 50% and 100% ethanol*

5a.4.3. Conformers of α-Synuclein at different concentrations of ethanol:

In **Figure 5a.4,** we can see the snapshots of α-Syn at 0%, 5%, 10%, 20%, 50% and 100% concentration of ethanol. We observed most of the residues to be in α-helical conformation with increasing concentration of ethanol.

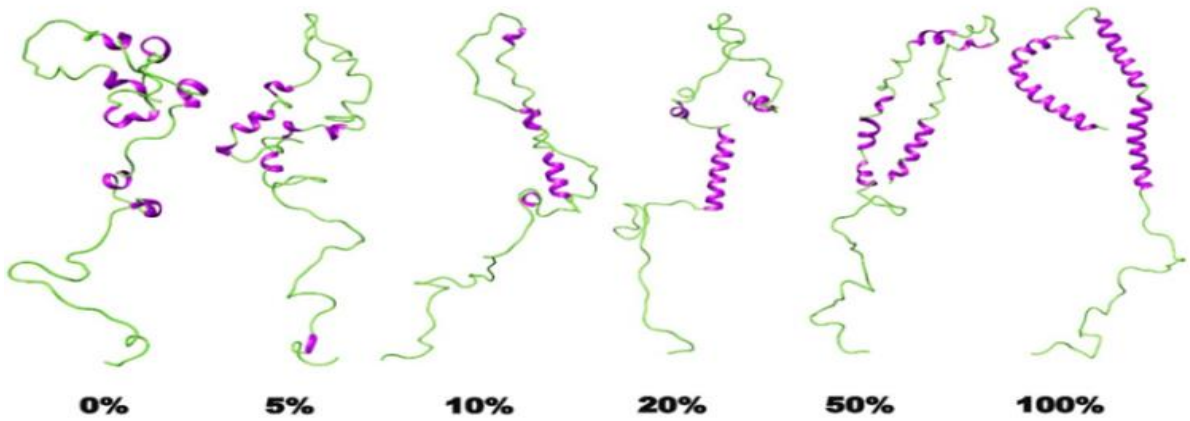

Figure 5a.4. *Snapshots of α-Syn conformers in presence of 0%, 5%, 10%, 20%, 50% and 100% ethanol during the time course of simulation*

5a.4.4. Analysis of Diffusion Co-efficient:

The values of diffusion coefficient for α-Syn in different concentrations of ethanol were summarized in the **Table 5a.2**. Diffusion coefficient values tends to decrease with increasing

concentration of ethanol but again at higher concentrations the corresponding values increase. This is so because of the shifts in the dielectric medium and structural changes of the molecule. In the beginning, the structure of α-Syn was more compact and its diffusion was affected by the presence of water molecules. But, gradually with an increase in ethanol concentration, the intermolecular interaction between water and α-Syn decreases. In 50% and 100% ethanol, the number of water molecules eventually decreases and becomes negligible, for which the attraction between the water molecules and the protein diminishes and thus the diffusion coefficient value escalates. This facilitates the sudden change in the pattern of the diffusion coefficient values with respect to increasing concentrations of ethanol.

Table 5a.2. *Diffusion Coefficient values of α-Syn in different concentrations of ethanol*

Concentrations of Ethanol	Diffusion Coefficient ($x10^{-10}$ cm^2/s)
0% Ethanol	0.5829
5% Ethanol	0.3703
10% Ethanol	0.2516
20% Ethanol	0.2148
50% Ethanol	0.2699
100% Ethanol	0.4446

5a.5. Conclusion:

In this work, the effect of molecular crowding on the conformational dynamics of α-Syn was studied. The conformational changes and fluctuations in α-Syn was found to decrease gradually with an increase in the concentration of ethanol, the crowding agent. We also noticed the solvent accessible surface area of α-Syn protein to decrease and the 3-D structure to become less compact at higher concentration of ethanol, which explains its decreasing tendency towards aggregation. Diffusion coefficient of α-Syn was found to be dependent on concentration of the ethanol, the crowding agent. With an increase in concentration of ethanol, the value of diffusion coefficient decreases initially but again increases at higher concentrations due to the change in dielectric medium, intermolecular interactions and structural changes in α-Syn. The intermolecular interactions between the solvent water molecules and α-Syn protein were found to decrease with an increase in concentration of ethanol. Our results show that along with excluded volume effect, the co-solute properties of crowded intracellular environment need to be considered to understand α-Syn dynamics in cells.

Chapter 5b

Screening of Druggable conformers of α-Synuclein using Molecular Dynamics Simulation

Screening of Druggable conformers of α-Synuclein using Molecular Dynamics Simulation

5b.1. Abstract:

IDP are becoming an engaging prospect for therapeutic intervention by small drug-like molecules. IDP structural binding pockets and their flexibility exists as a challenging target for standard druggable approaches. Hence, in this study, we have performed and identified the most probable druggable conformers from molecular dynamics simulation on α-Syn based on the structural parameters: R_g, SASA and the standard secondary structure content. We found the conformers showing lower solvent accessible surface area and higher secondary structure content of α-helical are defined to be suitable binding pockets for druggability.

5b.2. Introduction:

IDP exhibit prevalent key roles in biological processes of all diversified living organisms. IDP are broadly involved in crucial cellular activities, including regulation and signal transduction [384] and are also linked with a number of human diseases [385-387] such as in expression of cancer related proteins (p53, breast cancer protein BRCA-1/2) and other neurodegenerative disorders including the α-Syn and tau protein in AD [388]. IDP structural attributes of high flexibility and lack of stable secondary and tertiary structures, often engaged themselves at the hubs of protein-protein interaction networks and consequently associates with multiple partners [389-391]. The primary step of fibrillogenesis of IDP requires the stabilization of monomeric or oligomeric partially folded conformations as they are devoid of stable structure. As Statistically stated, 79% of malignancy related proteins and 57% of the distinguished cardiovascular disease related proteins are anticipated to contain disordered regions that are no longer than 30 residues in length [392, 393]. Therefore, IDP can be perceived as potential drug targets and are relied upon to play an active role in drug design [48, 394-398]. However, before conducting drug design on a specific protein it is crucial to evaluate its possibility to be a decent drug target. Also, presence of a suitable geometrical shaped cavities for ligand binding ("druggability"), acts as a crucial assessment problem in drug discovery [399]. The drug designs that target IDP are yet in their early stages [400] compared with the well-developed drug design pipelines that target proteins [401]. The cavity geometries of IDP are unique and are predicted to possess more binding cavities than ordered proteins of a similar length. In addition, from the literature review studies, it is evident that the cavities of IDP exerting greater surface areas and larger volumes shows higher druggability than those of ordered proteins. In addition, IDP must possess important

biological roles and establish its association with the specific disorder, which aids to drug designing towards IDP. Nonetheless, the optimism versus obstacles for drug design for IDP has been reported [388]. Although there are few limitations developed during drug designing targeted IDP of which major defaults were lack of efficient experimental screening strategies and determining specificity that impacts ligand- protein interactions. Most drugs target enzymes or cell surface receptors by regulating their functions, where small molecules can mimic the interactions made by their natural substrates [402]. Even though enzymes possess a certain degree of flexibility, their structures tend to fluctuate around equilibrium positions, making it easier to identify binding pockets and subsequently design drugs to fit in them. On the other hand, IDP exist as large ensembles of structures, where their amino acid chains can rapidly form multiple conformations, sometimes within microseconds. They exhibit large conformational fluctuations and no evidence of permanent binding pockets. This type of conformational feature does not present suitable cavities for small drug-like molecules to form stable interactions [48, 396, 403, 404]. IDP are frequently striking different postures. Allowing their highly dynamic nature into consideration, we have performed Molecular dynamics simulation on α-Syn protein [405], a typical IDP, to get a better sampling of conformers. The compactness of a protein which is measured as Radius of gyration (Rg) is known to affect the stability and folding rate of proteins [406]. In addition to this, recent studies have reported the use of compactness to define the binding pockets in a protein [407-409]. Some of the studies have highlighted the idea of considering compactness (Rg) of the protein or protein-ligand complexes for binding site prediction [407, 409]. Recent studies suggest that lower the Rg, the compactness of the ligand-protein complex is higher, causing the interactions between ligand and protein to be stronger [408]. Also, Rg depicts the significance of a more compact well-docked protein-ligand complex to be a better therapeutic agent [410, 411]. Structure-based prediction of ligand binding sites approaches have also been reported to focus on designing consensus that includes the shape of the input protein fold, expressed by its Rg, as one of its features [412]. In our study, we have performed 80 ns of MD simulation on α-Syn protein to analyze the conformational properties. From the MD simulation trajectory, the probable conformers of α-Syn having druggable features have been isolated based on the structural parameters; Rg, SASA and moderate standard secondary structure content.

5b.3. Materials and Methods:

5b.3.1. MD Simulation setup:

The MD study was carried out using a standard procedure, where the energy minimized structure of α-Syn was subjected to heating, equilibration and production dynamics. The system was gradually heated from 0-300 K in constant volume (NVT) conditions and then equilibration was conducted in NPT conditions (300 K and 1 atm pressure). To ensure correctness of our NPT simulation protocol, the density, temperature, pressure, energy and RMSD (Root Mean Square Deviation) graphs were plotted and analyzed (shown in **Figure 5b.1** and **Figure 5b.2**). Then 80 ns MD production run was carried out on the equilibrated structure using the Particle Mesh Ewald (PME) algorithm [337, 338] with the time step of 2 fs. To treat the nonbonding interactions (short-range electrostatic and van der Waals interactions) a cut off of 8 Å was used during the simulation while the long-range electrostatic interactions were treated with the PME method. All the bonds present in the system were constrained with the SHAKE algorithm [203]. The pressure and temperature (0.5 ps of heat bath and 0.2 ps of pressure relaxation) were held constant by the Berendsen weak coupling algorithm [343] throughout the simulation process. The trajectory analysis of the system was carried out using cpptraj program [305] from AmberTools.

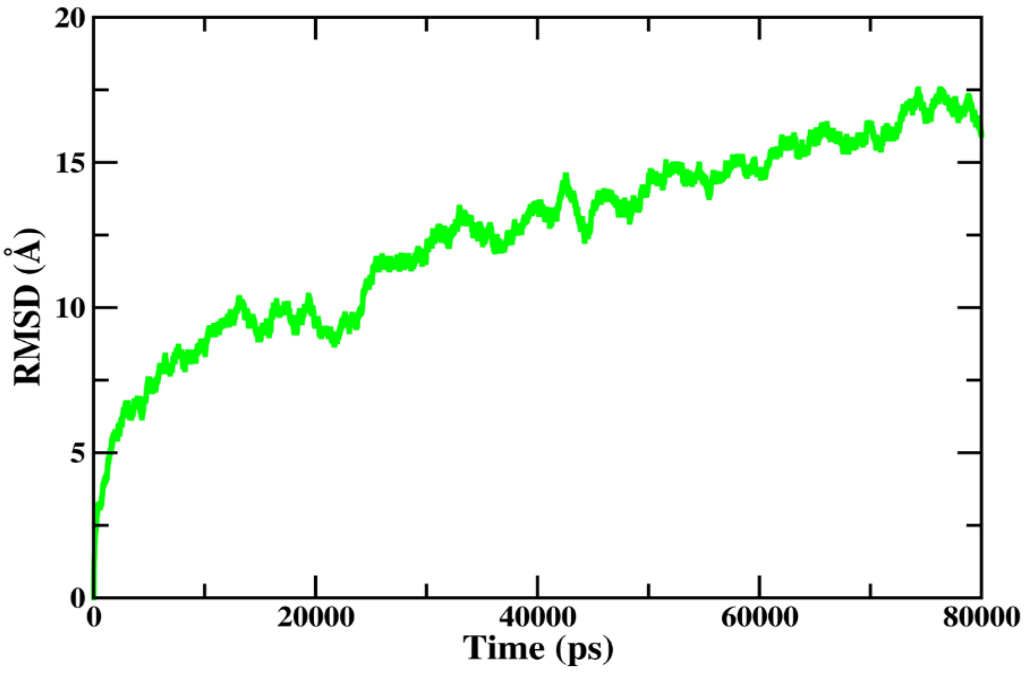

Figure 5b.1. *RMSD plot of α-Syn during MD simulation as function of simulation time*

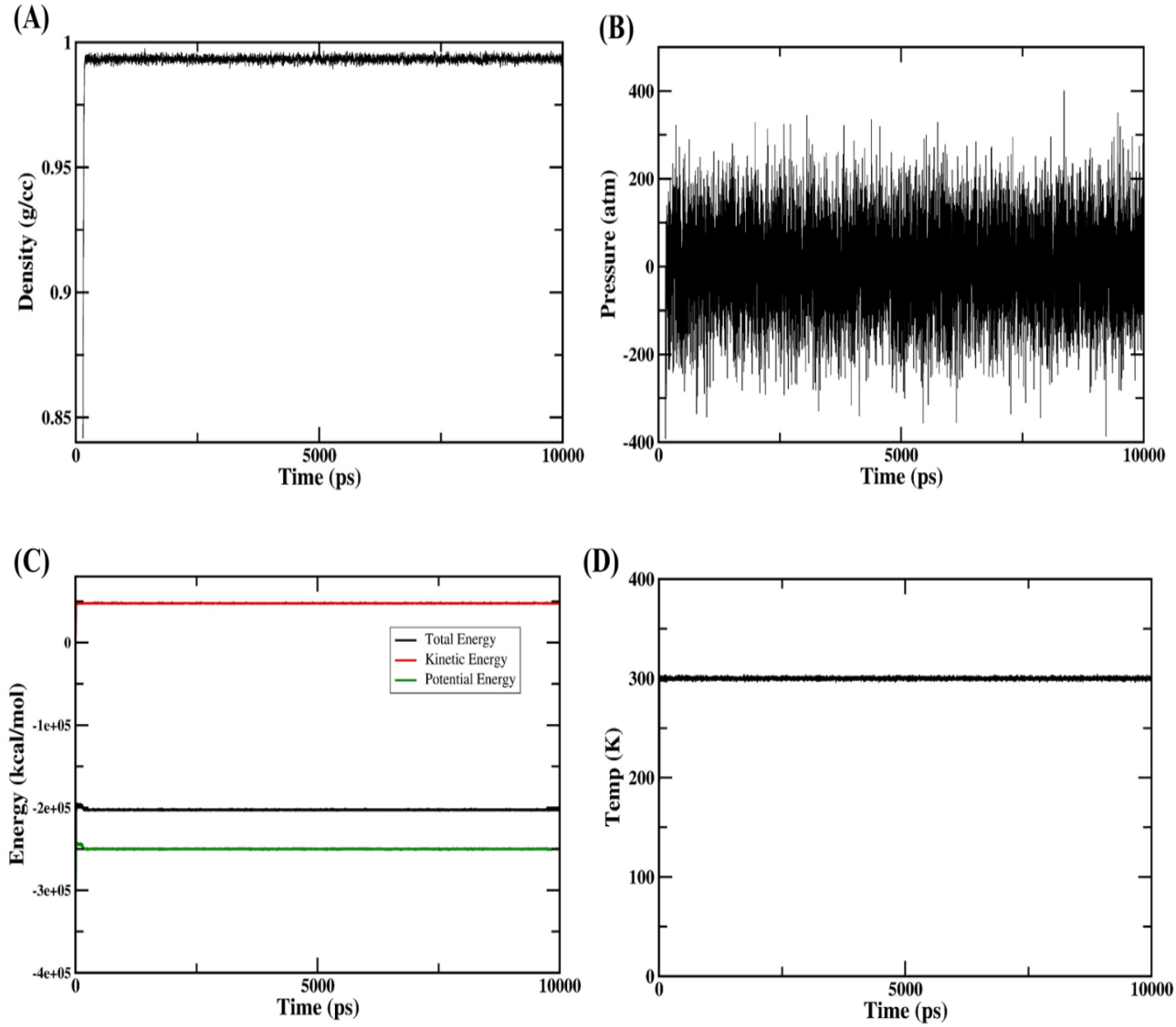

Figure 5b.2. *(A) Density, (B) Pressure, (C) Energy plots and (D) Temperature of α-Syn as a function of simulation time*

5b.3.2. Clustering of Conformers based on Radius of gyration:

In order to identify the druggable conformer of α-Syn protein from MD simulation trajectory, we have screened the conformers based on Rg values and grouped them into three clusters: L group (conformers having lower Rg values), M group (conformers having moderate Rg values) and H group (conformers having higher Rg values). For this study, we have pulled out the bottom five conformers depicted as L1-L5 from L group. Similarly, from M group and H group we have pulled out the top five conformers depicted as M1-M5 and H1-H5, respectively. To obtain information regarding the buried and exposed area present in each of these conformers, SASA analysis was carried out using cpptraj program [305].

5b.3.3. Prediction of Binding pockets:

The conformers in the clusters were analyzed using the online server tool CASTp [274] that detects, measures and provides a detailed characterization of the binding pockets on the surface of the proteins as well as the voids in the interior of proteins. Usually, these surface pockets and voids that correlate with binding activities are the concave regions of the proteins. CASTp uses the α-shape and the pocket algorithm developed in computational geometry to define and measure the surface pockets and voids in proteins. This server describes the surface pockets as concave regions of proteins with binding sites at the opening. These pockets also allow easy access to water molecules from the exterior.

5b.4. Results and Discussions:

In this study, we have screened the conformers of α-Syn protein from the MD simulation trajectory that exhibit well defined binding pockets necessary for druggability.

5b.4.1. Radius of gyration Analysis:

To investigate the compactness of α-Syn protein during the simulation, radius of gyration was analyzed. Information regarding the overall shape and size of the molecule can be gleaned from R_g. The radius of gyration analysis for α-Syn protein as a function of simulation time is shown in **Figure 5b.3**. The R_g value is known to affect both the stability and folding rate of a protein. From **Figure 5b.3**, we can infer that the R_g value of α-Syn was found to be oscillating within the range of 41 Å to 48 Å during the course of simulation. In order to isolate the probable conformers of α-Syn featuring druggability, the conformers from the MD simulation trajectory were clustered according to their R_g values. Conformers L1-L5, M1-M5 and H1-H5 were selected from the clusters of lower, moderate and higher values of R_g, respectively.

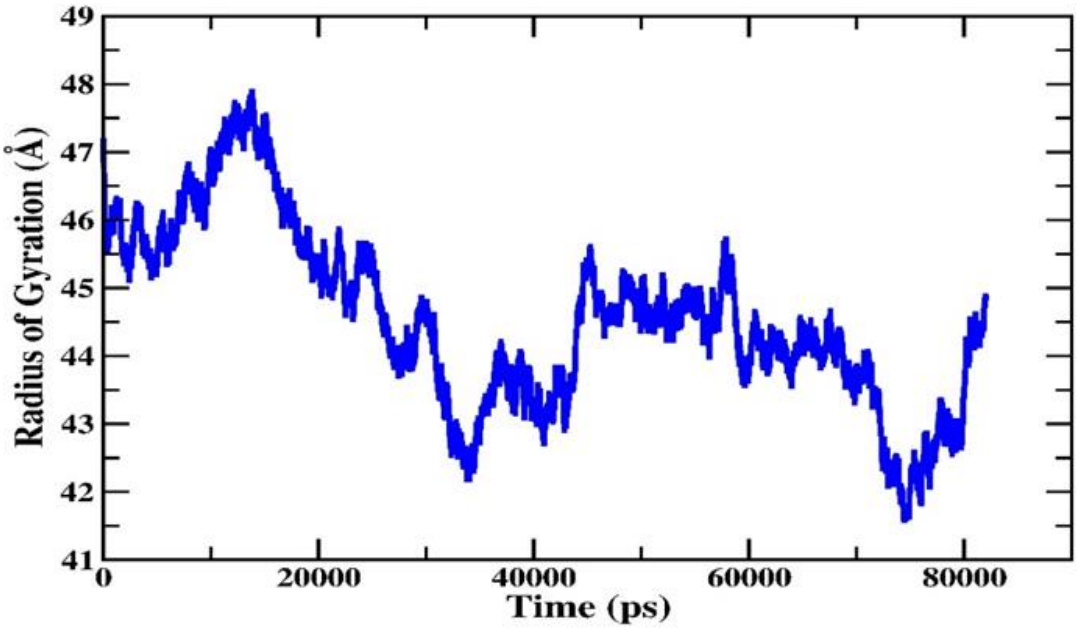

Figure 5b.3. *Radius of Gyration analysis for α-Syn as a function of simulation time*

5b.4.2. Solvent accessible surface area Analysis:

In order to investigate the absolute details about the mobility of flexible regions in α-Syn protein, we calculated SASA from MD simulation trajectory using cpptraj program. The results were depicted in **Figure 5b.4**. From **Figure 5b.4**, we can infer that the SASA value of α-Syn takes the value in the range of 13400 $Å^2$ to 14800 $Å^2$. Hence, it depicted that the mobility of flexible regions in α-Syn protein was observed in the range of 13400 $Å^2$ to 14800 $Å^2$. It can be correlated with the **Table 5b.1** with the number of R_g and binding pockets.

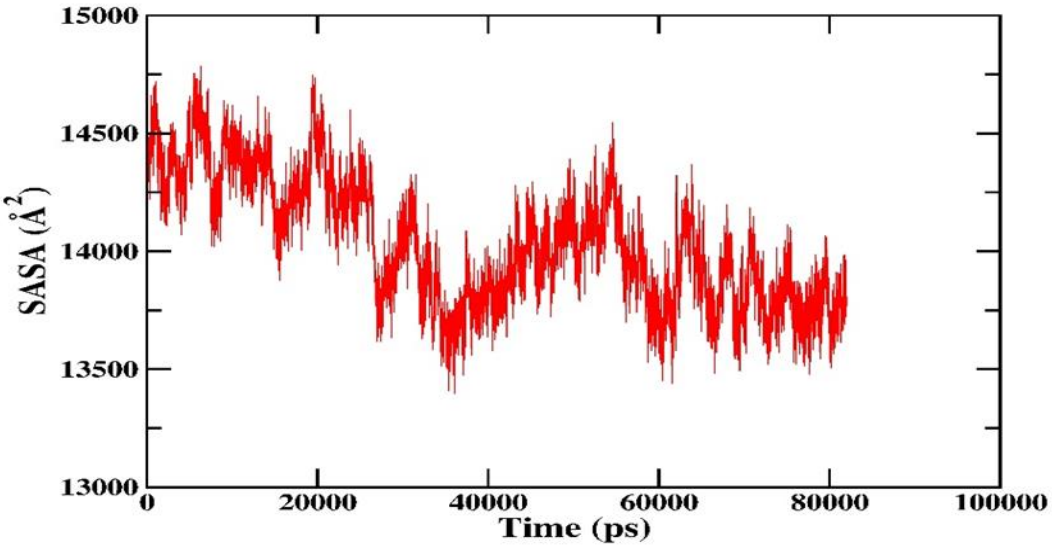

Figure 5b.4. *SASA analysis for α-Syn as function of simulation time*

5b.4.3. Binding Pocket Analysis:

Binding pockets in the screened conformers of α-Syn having lower (L1-L5), moderate R_g (M1-M5) and higher R_g (H1-H5) values have been predicted with the help of CASTp server and results were depicted in **Figure 5b.5.** In **Table 5b.1**, we have summarized the R_g, SASA and the number of binding pockets of the corresponding screened conformers of α-Syn. From **Table 5b.1**, we observe the number of binding pockets to be more in the conformers having lower R_g values than conformers having higher R_g values. Also, we notice the conformers having lesser SASA values to contain more binding pockets. Hence, we observe that among H, M and L group, the conformers under Group L contain a greater number of well-defined binding pockets. From these observations, we can infer that R_g and SASA value of the protein may be considered as critical aspects for identifying the conformers having druggable features.

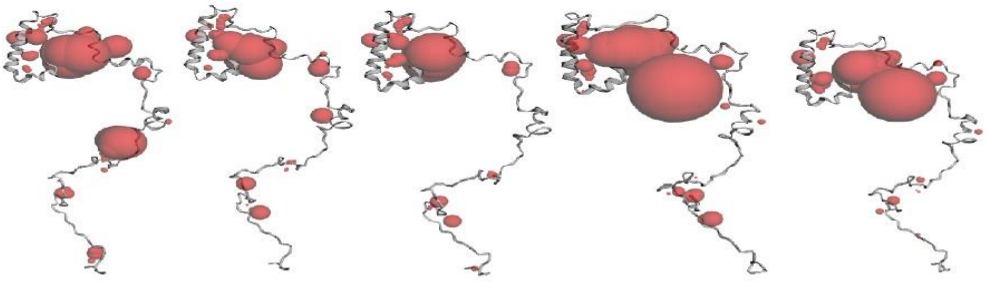

(A)

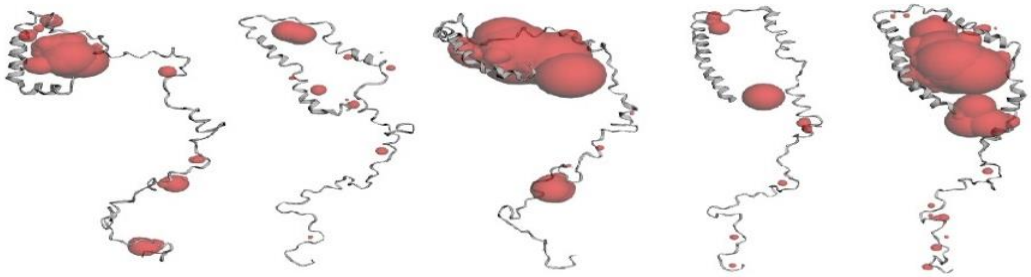

(B)

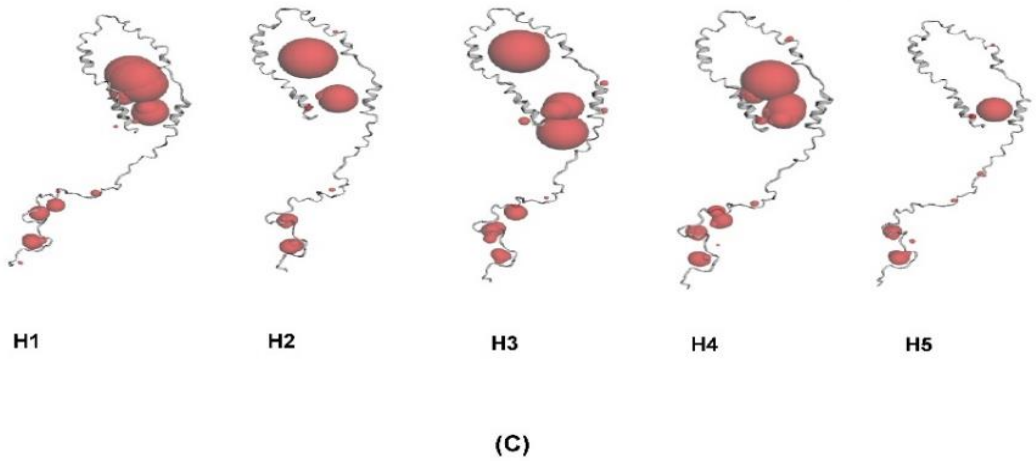

Figure 5b.5. *Binding pocket analysis for the conformers of α-Syn having (A) Lower R_g values (B) Moderate R_g values. (C) Higher R_g values*

Table 5b.1. *R_g, SASA and Number of binding pockets for the screened conformers of α-Syn having lower, middle and higher R_g values*

CONFORMERS	Rg VALUES (Å)	SASA VALUES (Å^2)	NUMBER OF BINDING POCKETS
L1	41.582	13692.33	15
L2	41.588	13748.63	17
L3	41.597	13728.49	11
L4	41.599	13791.03	19
L5	41.603	13798.73	16
M1	42.997	13973.61	9
M2	43.999	13804.06	10
M3	44.998	13862.44	11
M4	45.973	14255.19	7
M5	46.041	14655.89	15
H1	47.895	14494.96	11
H2	47.868	14477.31	7
H3	47.868	14341.28	11
H4	47.864	14377.58	9
H5	47.855	14415.70	8

5b.4.4. Secondary Structural Analysis:

The Secondary structure analysis was carried out using the Kabsch and Sander algorithm [295] incorporated in their DSSP program. The results were plotted in **Figure 5b.6**. The plot shows the structural variation of each residue during the time course of the simulation. From **Figure 5b.6**, we observe that α-helix secondary structure was mostly retained in the N-terminal region of the protein while in the NAC and C-terminal region there were rapid transitions from one secondary structure to another.

We have also calculated the percentage of individual secondary structure content across the screened conformers using YASARA software [257]. Considering both the secondary structure content and number of binding pockets in the screened conformers, we have summarized the results in **Table 5b.2**. From **Table 5b.2**, it can be observed that L4 in spite of having a comparatively higher Rg value than the other conformers in that group, was estimated to contain relatively a greater number of binding pockets. This is the same for M5 and H3 under the group M and H respectively. We found that in all these conformers (L4, M5 and H3), the percentage of α-helical secondary structure content is relatively more than the other conformers in the corresponding groups. From these observations, we can infer that in addition to Rg and SASA, the percentage of the standard secondary structure content, especially, α helical portion of the protein to play a significant role in influencing the occurrence of number of binding pockets. The additional information about the geometry (area and volume), number of residues and atoms involved in the binding pockets of all the screened conformers have been summarized in **Table 5b.3**. The cavities of IDP are more likely to be composed of a single segment and have larger surface areas and volumes than cavities of ordered proteins [388]. Therefore, conformers with lower Rg value, lesser solvent accessible surface area and higher standard secondary structure content are more preferable to possess druggable features.

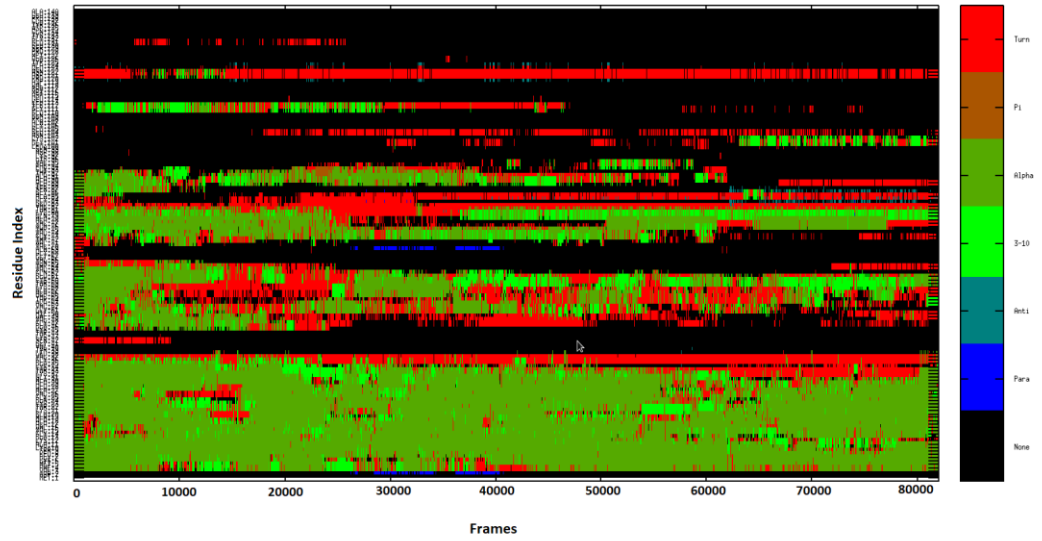

Figure 5b.6. *The evolution of secondary structure evaluated using DSSP is shown for α-Syn. Y-axis depicts residues and X-axis depicts time frames during the course of MD simulation. The secondary structure components of α-Syn are color-coded as shown in the panel.*

Table 5b.2*. Secondary structure content and the Number of Binding Pockets for the conformers of α-Syn having lower, middle and higher R_g values*

CONFORMERS	SECONDARY STRUCTURES				Number of binding pockets
	α-helix %	β-sheet %	turn %	Coil %	
L1	21.4	0.0	14.3	64.3	15
L2	22.1	0.0	14.3	60.0	17
L3	17.9	0.0	22.9	59.3	11
L4	22.9	0.0	14.3	62.9	19
L5	17.9	0.0	14.3	65.0	16
M1	19.3	0.0	20.0	60.7	9
M2	20.7	0.0	22.9	52.9	10
M3	20.7	0.0	20.0	59.3	11
M4	26.4	0.0	11.4	59.3	7
M5	40.0	0.0	11.4	48.6	15
H1	12.9	0.0	31.4	55.7	11
H2	11.4	0.0	40.0	48.6	7
H3	21.4	0.0	25.7	52.9	11
H4	15.7	0.0	34.3	50.0	9
H5	12.1	0.0	25.7	59.3	8

Table 5b.3. *Binding Pocket Information for all the screened conformers of α-Syn*

BINDING POCKET INFORMATION: L1				
POCKET ID	AREA (SA)	VOLUME (SA)	NUMBER OF RESIDUES	NUMBER OF ATOMS
1	193.56	984.96	12	46
2	158.94	484.77	12	41
3	19.93	60.39	4	7
4	21.62	14.97	4	13
5	12.98	11.36	5	14
6	17.84	10.64	4	13
7	16.53	8.49	4	13
8	10.52	7.73	5	8
9	19.52	7.36	6	13
10	26.98	5.26	8	20
11	7.57	0.93	6	11
12	1.42	0.25	3	5
13	1.38	0.16	4	4
14	1.51	0.14	4	7
15	0.38	0.00	4	6
BINDING POCKET INFORMATION: L2				
POCKET ID	AREA (SA)	VOLUME (SA)	NUMBER OF RESIDUES	NUMBER OF ATOMS
1	178.50	749.40	16	50
2	33.16	17.73	5	13
3	27.29	14.46	5	14
4	16.42	14.45	4	11
5	13.94	8.26	4	11
6	5.37	6.53	5	7
7	27.47	4.56	8	21
8	10.64	4.55	4	6

9	2.71	0.42	5	7
10	3.76	0.40	3	6
11	4.00	0.24	6	11
12	0.62	0.06	3	4
13	0.78	0.02	4	8
14	0.36	0.00	5	6
15	0.01	0.00	4	5
16	0.01	0.00	3	4
17	0.00	0.00	3	4

BINDING POCKET INFORMATION: L3

POCKET ID	AREA (SA)	VOLUME (SA)	NUMBER OF RESIDUES	NUMBER OF ATOMS
1	137.68	733.85	10	30
2	50.50	18.02	10	33
3	16.15	11.97	4	10
4	19.01	11.88	4	12
5	26.05	9.91	5	12
6	16.39	8.25	5	13
7	9.65	6.58	4	7
8	5.74	0.75	6	12
9	5.83	0.52	6	10
10	0.95	0.11	3	4
11	0.06	0.00	4	5

BINDING POCKET INFORMATION: L4

POCKET ID	AREA (SA)	VOLUME (SA)	NUMBER OF RESIDUES	NUMBER OF ATOMS
1	143.66	770.42	14	32
2	12.25	286.00	5	5
3	12.62	8.27	4	10

4	27.92	7.15	7	15
5	12.39	6.77	5	8
6	2.70	6.51	4	9
7	5.85	5.12	4	6
8	9.47	4.18	4	7
9	20.99	3.85	8	20
10	9.38	2.41	4	8
11	3.64	2.00	3	5
12	0.85	0.15	3	4
13	1.43	0.11	4	6
14	0.97	0.08	4	5
15	0.19	0.00	3	5
16	0.14	0.00	3	4
17	0.09	0.00	4	5
18	0.06	0.00	3	4
19	0.00	0.00	4	4
BINDING POCKET INFORMATION: L5				
POCKET ID	AREA (SA)	VOLUME (SA)	NUMBER OF RESIDUES	NUMBER OF ATOMS
1	178.30	1063.89	14	41
2	33.12	21.01	6	13
3	23.05	15.25	4	15
4	33.81	13.09	7	20
5	8.47	9.83	4	7
6	23.73	2.49	8	21
7	3.74	0.68	3	6
8	4.25	0.50	5	10
9	0.71	0.17	2	4
10	1.51	0.16	4	4
11	0.45	0.03	4	4
12	0.21	0.01	3	4
13	0.21	0.00	3	5

14	0.20	0.00	3	4
15	0.05	0.00	3	4
16	0.03	0.00	4	4

BINDING POCKET INFORMATION: M1				
POCKET ID	AREA (SA)	VOLUME (SA)	NUMBER OF RESIDUES	NUMBER OF ATOMS
1	252.50	864.36	18	46
2	25.87	20.37	6	18
3	12.76	14.29	7	13
4	25.48	9.64	7	14
5	6.69	2.46	4	9
6	8.18	2.35	4	10
7	6.66	0.60	6	14
8	0.15	0.03	3	4
9	13.24	-0.77	4	10

BINDING POCKET INFORMATION: M2				
POCKET ID	AREA (SA)	VOLUME (SA)	NUMBER OF RESIDUES	NUMBER OF ATOMS
1	50.09	88.77	7	16
2	6.23	2.62	4	6
3	6.86	1.56	7	10
4	5.47	1.29	5	7
5	2.72	0.43	4	6
6	1.23	0.25	4	7
7	2.78	0.13	4	6
8	1.92	0.12	3	5
9	0.40	0.00	3	4
10	0.13	0.00	3	6

BINDING POCKET INFORMATION: M3				
POCKET ID	AREA (SA)	VOLUME (SA)	NUMBER OF RESIDUES	NUMBER OF ATOMS
1	473.13	2505.87	26	88
2	16.50	79.05	4	7
3	48.09	78.88	7	14
4	-0.29	0.12	3	6
5	0.81	0.11	3	4
6	0.62	0.03	5	5
7	0.37	0.01	4	6
8	0.39	0.00	4	5
9	0.12	0.00	3	5
10	0.01	0.00	3	4
11	0.01	0.00	3	4
BINDING POCKET INFORMATION: M4				
POCKET ID	AREA (SA)	VOLUME (SA)	NUMBER OF RESIDUES	NUMBER OF ATOMS
1	15.61	77.29	4	5
2	29.58	12.04	6	17
3	27.65	7.96	6	14
4	4.24	3.45	3	6
5	6.73	1.04	4	6
6	-0.88	0.84	4	7
7	2.45	0.35	4	4
BINDING POCKET INFORMATION: M5				
POCKET ID	AREA (SA)	VOLUME (SA)	NUMBER OF RESIDUES	NUMBER OF ATOMS
1	307.12	2134.89	22	64
2	152.19	506.34	11	33
3	44.26	104.99	7	14

4	16.62	5.30	7	16
5	17.33	2.23	7	16
6	1.63	0.37	3	5
7	1.42	0.24	4	5
8	0.45	0.21	2	4
9	1.22	0.17	3	5
10	2.06	0.15	4	7
11	1.30	0.10	4	7
12	1.43	0.04	4	7
13	0.30	0.01	4	5
14	0.51	0.00	3	5
15	0.11	0.00	4	4

BINDING POCKET INFORMATION: H1				
POCKET ID	AREA (SA)	VOLUME (SA)	NUMBER OF RESIDUES	NUMBER OF ATOMS
1	12.49	124.01	4	6
2	25.51	122.40	4	9
3	57.36	70.22	8	22
4	21.98	46.99	5	10
5	16.38	14.53	4	8
6	2.53	3.78	3	5
7	9.26	1.16	4	10
8	1.89	0.10	4	6
9	0.74	0.04	2	4
10	0.59	0.04	2	4
11	0.62	0.03	4	6
BINDING POCKET INFORMATION: H2				
POCKET ID	AREA (SA)	VOLUME (SA)	NUMBER OF RESIDUES	NUMBER OF ATOMS
1	27.44	135.05	4	9
2	50.20	58.95	8	21

3	49.60	39.36	8	17
4	1.90	28.35	3	4
5	1.04	0.22	2	4
6	0.41	0.05	2	4
7	0.79	0.04	5	5

BINDING POCKET INFORMATION: H3				
POCKET ID	AREA (SA)	VOLUME (SA)	NUMBER OF RESIDUES	NUMBER OF ATOMS
1	15.33	157.75	5	7
2	39.06	128.30	5	12
3	13.80	61.39	4	9
4	71.76	60.45	9	23
5	15.94	29.62	4	5
6	21.85	19.34	6	13
7	3.87	1.18	3	6
8	2.45	0.35	4	11
9	0.92	0.04	3	8
10	0.29	0.01	5	6
11	2.64	-0.38	4	6

BINDING POCKET INFORMATION: H4				
POCKET ID	AREA (SA)	VOLUME (SA)	NUMBER OF RESIDUES	NUMBER OF ATOMS
1	52.79	191.90	5	15
2	26.01	75.72	6	12
3	45.78	47.28	6	15
4	43.92	42.65	7	15
5	50.52	41.42	8	18
6	5.77	1.87	4	7
7	4.45	0.51	6	10
8	4.42	0.07	4	9
9	0.24	0.00	3	5

BINDING POCKET INFORMATION: H5				
POCKET ID	AREA (SA)	VOLUME (SA)	NUMBER OF RESIDUES	NUMBER OF ATOMS
1	17.70	96.24	4	6
2	56.92	56.07	7	20
3	60.50	48.41	8	21
4	3.47	0.84	3	9
5	1.83	0.30	3	7
6	1.35	0.20	3	5
7	1.23	0.08	3	8
8	0.92	0.03	4	5

5b.5. Conclusion:

In conclusion, we have demonstrated here that isolation of the most probable conformer of α-Syn from structural MD analysis based on some critical aspects that emphasizes on its nature of druggabilty as a potential drug target. Our observations have supported that conformers having lower values of Rg have definitely greater number of binding pockets. With higher compactness of the structure, greater cavities are observed which are aided by the conformers. However, this is not the only factor that is solely responsible for the druggable nature of the protein molecule. Compactness coupled with the solvent accessible surface areas of the conformers and also their secondary structure content, are equally crucial attributes. Also, the parameters of the binding pockets in a protein molecule, serve as an essential element to be considered for drug design approaches. In this study we have identified conformers of α-Syn containing druggable features that can serve as an input in designing drug like molecules. Our findings interpreted an idealistic insight on defining the druggability of α-Syn that can be anticipated for which it will be considered as a preferable target in drug discovery initiatives in the future. From the above references studied and to the best of our knowledge, the proposed strategy may be used as a potential method to characterize druggability and can be generalized to overcome the obstacles for drug design of other IDP as well.